Zero-Shot Accurate mmWave Antenna Array Calibration in the Wild

Oveys Delafrooz Noroozi*
University of California, Santa Barbara
oveys@ucsb.edu

Heyu Guo*
Princeton University
hg9046@princeton.edu

Ruiyi Shen
Princeton University
ruiyishen@princeton.edu

Zijian Shao
Princeton University
zs9193@princeton.edu

Haoze Chen
Princeton University
hc9271@princeton.edu

Kaushik Sengupta
Princeton University
kaushiks@princeton.edu

Yasaman Ghasempour
Princeton University
ghasempour@princeton.edu

Upamanyu Madhow
University of California, Santa Barbara
madhow@ucsb.edu

ABSTRACT

mmWave antenna array calibration is a necessary yet tedious and costly process in manufacturing to capture the non-idealities in phased arrays, in order to obtain codebooks for accurate and stable beam steering. Unfortunately, predefined codebooks provided by manufacturers to steer beams in a given set of directions do not support the arbitrary beam shapes required for various mmWave communication, sensing, and security applications. To create arbitrary beam patterns, one needs to first find the unknown calibration vector for the particular phased array in use. In this paper, we introduce *EiCal*, a novel zero-shot technique that leverages the beamforming codebook advertised by the manufacturer to extract the calibration vector at zero cost (i.e., with no additional measurements). The key idea is that the unknown desired calibration vector can be obtained via an appropriately designed eigen-decomposition of the given codebook. We experimentally demonstrate the efficacy of *EiCal* on a 60 GHz mmWave array for two scenarios: angle estimation using compressive pseudorandom beams, and simultaneous steering of beams and nulls. Our results also point to potential simplifications in the calibration process at the manufacturer.

CCS CONCEPTS

• **Hardware** → **Beamforming**.

KEYWORDS

Calibration, Antenna arrays, mmWave, Zero-shot

ACM Reference Format:
Oveys Delafrooz Noroozi, Heyu Guo, Ruiyi Shen, Zijian Shao, Haoze Chen, Kaushik Sengupta, Yasaman Ghasempour, and Upamanyu Madhow. 2024. Zero-Shot Accurate mmWave Antenna Array Calibration in the Wild. In *The 30th Annual International Conference on Mobile Computing and Networking (ACM MobiCom '24), November 18–22, 2024, Washington D.C., DC, USA.* ACM, New York, NY, USA, 8 pages. https://doi.org/10.1145/3636534.3697323

1 INTRODUCTION

Phased arrays play a critical role in mmWave communication and sensing [14, 15]. The small carrier wavelengths in the mmWave bands enable miniaturization of antenna arrays with a large number of elements, while RFIC (radio frequency integrated circuit) design is simplified by connecting a single RF chain to the antenna elements, with separate amplitude and/or phase control for each element. A variety of beam patterns optimized for different communication and sensing settings can be formed by such arrays, including directional beams for providing high gain in a given direction, nulls for reducing interference, and pseudorandom beams for compressive sensing. The amplitude/phase control to synthesize a given beam pattern requires knowledge of the relative geometry and the relative local oscillator phases at the different array elements.

*Both authors contributed equally to this research.

ACM MobiCom '24, November 18–22, 2024, Washington D.C., DC, USA

ACM ISBN 979-8-4007-0489-5/24/11
https://doi.org/10.1145/3636534.3697323

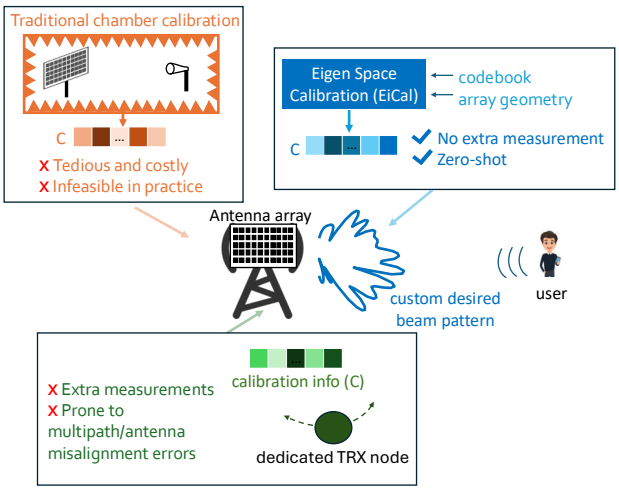

Figure 1: Overview of EiCal: Zero-shot accurate mmWave antenna array calibration.

While the physical geometry of array elements is usually accurately known (e.g., a linear array with equally spaced elements), the relative phases between the elements are often less predictable for many RF designs (e.g., due to variations in the lengths of the transmission lines in the circuit board connecting the RFIC to the antennas), and requires calibration. A manufacturer may, for example, provide a "codebook" based on a large number of controlled measurements in an anechoic chamber, with each entry in the codebook specifying the amplitude/phase controls required to form a beam towards a given direction. However, such codebooks do not tell us how to create other kinds of beam patterns, such as forming nulls in addition to beams, or compressive beam patterns with pseudorandom phases which can be used for sensing.

For an antenna array with known geometry, if the amplitude/phase relationships between antennas (prior to applying any controls) are stable, and there are no difficult-to-model effects such as direction-dependent mutual coupling between elements, then we simply need to determine a single calibration vector summarizing these relationships in order to synthesize any such beam pattern. Indeed, the lack of such calibration information is one of the major bottlenecks for exploiting already deployed infrastructure in the wild for various sensing use cases. While, in principle, a dedicated mobile node can be used in the wild for calibration purposes (albeit via exhaustive time-consuming measurements), the uncontrolled nature of the environment (e.g., multipath, slight antenna misalignment) prevents an accurate estimation in practice.

In this paper, we show that an accurate calibration vector can be extracted from an existing codebook via eigen-analysis *without additional measurements,* and to experimentally demonstrate on a COTS 60 GHz hardware (see Section 4) that such a calibration vector indeed suffices to produce a variety of beam patterns beyond simple beamforming in a given direction. While we demonstrate our calibration method on a specific hardware platform, it applies to any phased array for which a large enough number of beamforming codebook entries are known. Our results also show that the number of codebook entries can be significantly reduced without compromising the quality of the calibration vector that we extract from it. An overview of how our proposed "zero shot" approach, which we term *EiCal*, relates to the state of the art, is depicted in Fig. 1.

We summarize our contributions as follows:

- We present *EiCal*, a method for obtaining an array calibration vector in computationally efficient fashion by eigen-analysis of an existing codebook, without requiring any additional measurements.
- We experimentally demonstrate that the single calibration vector produced by EiCal indeed suffices for synthesizing a variety of beam patterns, including for compressive angle estimation and for null formation. We use 60 GHz Sivers radio [9] as our evaluation platform.
- Our experiments demonstrate that, for the compressive sensing and null forming tasks considered, EiCal performs better than baselines such as recently proposed calibration techniques that employ additional measurements.
- We show that the accuracy of calibration quickly plateaus in the number of codebook entries needed. This indicates that the number of calibration measurements required can be significantly reduced from what is currently provided, potentially reducing the burden of calibration in the manufacturing process.

2 PRIMER

We now discuss our model for calibration. While the approach is general, we illustrate it for linear array with uniformly spaced elements, as depicted in Fig. 2. For a calibrated array, in order to create a constructive pattern toward the angle of θ_k (relative to the broadside), we must apply a relative phase shift of $\Omega_k = \frac{2\pi d sin(\theta_k)}{\lambda}$ between neighboring elements. This corresponds to a $N\times 1$ *nominal* steering vector

$$\mathbf{a}_{\text{Nominal}}(\Omega_k) = \left[1\, e^{-j\Omega_k} \cdots e^{-j(N-1)\Omega_k}\right]^T, \Omega_k = \frac{2\pi d sin(\theta_k)}{\lambda}, \quad (1)$$

where N is the number of antenna elements.

Thus, in order to steer the beam towards K pre-defined angles, $\{\theta_1, \theta_2, ..., \theta_K\}$, the *nominal* codebook for an ideally calibrated array is given by the $N \times K$ matrix

$$\mathbf{A}_{\text{Nominal}} = [\mathbf{a}_{\text{Nominal}}(\Omega_1)\, \mathbf{a}_{\text{Nominal}}(\Omega_2) \cdots \mathbf{a}_{\text{Nominal}}(\Omega_K)], \quad (2)$$

In practice, however, the codebook provided by the manufacturer differs from the above theoretical calculation. The

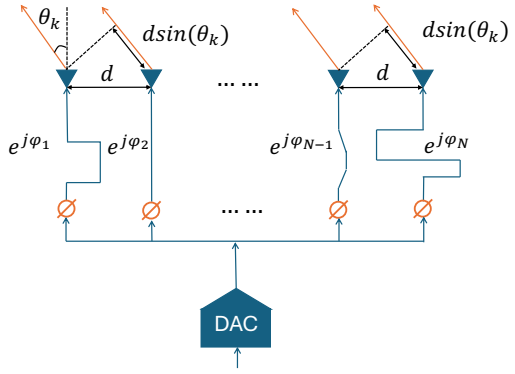

Figure 2: Non-idealities in the phased array circuitry including unequal transmission lines necessitates calibration.

reason behind this discrepancy is multi-fold: first, most practical phase shifters have limited resolutions and hence quantization is needed. Second, imperfections in the circuitry, such as unequal lengths of transmission lines between different antennas and their corresponding phase shifters, induce additional phase shifts not accounted for in Eq. (2). Thus, for an *a priori* uncalibrated array to be used for beamforming, a typical procedure is for the manufacturer to determine the weight vectors for a pre-defined desired steering codebook through extensive measurements in an anechoic chamber. Let $\mathbf{a}_{\text{Advertised}}(\Omega_k)$ denote the weight vector required to steer along direction θ_k, as determined by such measurements. For the pre-defined set of steering directions $\{\theta_1, \theta_2, ..., \theta_K\}$, the *advertised* codebook contains these steering vectors as columns:

$$\mathbf{A}_{\text{Advertised}} = [\mathbf{a}_{\text{Advertised}}(\Omega_1)\, \mathbf{a}_{\text{Advertised}}(\Omega_2)\, \cdots\, \mathbf{a}_{\text{Advertised}}(\Omega_K)]\,. \tag{3}$$

This is then shared with customers and embedded in the control unit of the antenna front end. If we are only interested in synthesizing directional beams in a quantized set of directions, such a codebook provides a completely general approach to modeling non-idealities in the array hardware, including not only variations in amplitude and phase references across array elements, but also more complex effects such as mutual coupling between elements, which can actually depend on the direction of arrival/departure [1]. However, the advertised codebook does not provide the information needed to synthesize a richer set of beam patterns, such as those required for compressive sensing or null formation.

Our approach to calibration is based on the hypothesis that we can ignore effects such as mutual coupling for the simple linear arrays employed in the COTS hardware that we work with, and that the dominant non-idealities are the variation in amplitude and phase references across elements, along with the inaccuracy incurred due to quantization of the weights in the advertised codebook. This hypothesis is validated by our experimental results, which show that our approach accurately reproduces the advertised codebook entries, and enables accurate compressive sensing and null formation. Under this model, calibration can be accomplished by finding a single N-element calibration vector $\mathbf{C} \in \mathbb{C}^{N\times 1}$, with the advertised weight vector for beamforming in the kth direction relating to the corresponding nominal weight vector as follows:

$$\mathbf{a}_{\text{Advertised}}(\Omega_k) = Q\left(\alpha_k\, \mathbf{C} \odot \mathbf{a}_{\text{Nominal}}(\Omega_k)\right)\ ,\ k = 1, ..., K \tag{4}$$

where $\odot$ represents an element-wise product, α_k represents an arbitrary complex scalar that can vary for different beam directions, and $Q(\cdot)$ is a quantization function that quantizes the phase of its input. For instance, commercially available 60 GHz arrays have 6-bit phase shifters [9].

In the next section, we provide a computationally efficient approach for estimating the calibration vector $\mathbf{C}$ given the advertised codebook $\mathbf{A}_{\text{Advertised}}$. Once this is accomplished, in order to synthesize a desired beam pattern, we use the idealized array model to obtain a nominal weight vector, and then adjust it using the calibration vector. The final beam pattern is, of course, a product of this synthesized beam pattern with the radiation pattern for a single element.

3 EICAL DESIGN

In this section, we derive EiCal, a zero-shot measurement-free strategy for extracting a calibration vector. From (4) that the k^{th} columns of the $\mathbf{A}_{\text{Advertised}}$ and $\mathbf{A}_{\text{nominal}}$ matrices defined in Section 2 can be related as follows:

$$\mathbf{a}_{\text{Advertised}}(\Omega_k) = \alpha_k \mathbf{C} \odot \mathbf{a}_{\text{Nominal}}(\Omega_k) + \mathbf{n}_k,\ k = 1, ..., K \tag{5}$$

where $\mathbf{n}_k$ is a $N \times 1$ noise vector modeling quantization noise and any other model mismatches. We can therefore recover K noisy, scaled copies of the calibration vector by "taking out" the nominal array responses from the advertised array responses as follows:

$$\mathbf{a}_{\text{Advertised}}(\Omega_k) \odot \mathbf{a}^*_{\text{Nominal}}(\Omega_k) = \alpha_k \mathbf{C} + \tilde{\mathbf{n}}_k,\ k = 1, ..., K \tag{6}$$

where $\tilde{\mathbf{n}}_k = \mathbf{n}_k \odot \mathbf{a}^*_{\text{Nominal}}(\Omega_k)$ is a transformed noise vector.

The K scaled, noisy copies of the calibration vector obtained in (6) are easily seen to be the columns of the matrix obtained by entry-by-entry multiplication of the advertised codebook with the complex conjugate of the nominal codebook:

$$\mathbf{P} = \mathbf{A}_{\text{Advertised}} \odot \mathbf{A}^*_{\text{Nominal}} = (\alpha_1 \mathbf{C} .... \alpha_K \mathbf{C}) + \tilde{\mathbf{N}} \tag{7}$$

where the noise matrix $\tilde{\mathbf{N}}$ contains as columns the transformed noise vectors $\tilde{\mathbf{n}}_k$, $k = 1, ..., K$.

Ignoring the noise term in (7), the columns in $\mathbf{P}$ are all multiples of the same vector $\mathbf{C}$, corresponding to a matrix of rank one. We can therefore obtain an estimate of $\mathbf{C}$ via a rank one approximation of the noisy matrix $\mathbf{P}$. The best rank one approximation of a matrix is the largest "eigenmode" in the singular value decomposition (SVD) of $\mathbf{P}$ [5]. The SVD for the $N \times K$ matrix $\mathbf{P}$ takes the form:

$$\mathbf{P} = \mathbf{U}\, \text{diag}\{\sigma_1, ..., \sigma_m\}\mathbf{V}^H = \sum_{i=1}^{m} \sigma_i \mathbf{u}_i \mathbf{v}_i^H \tag{8}$$

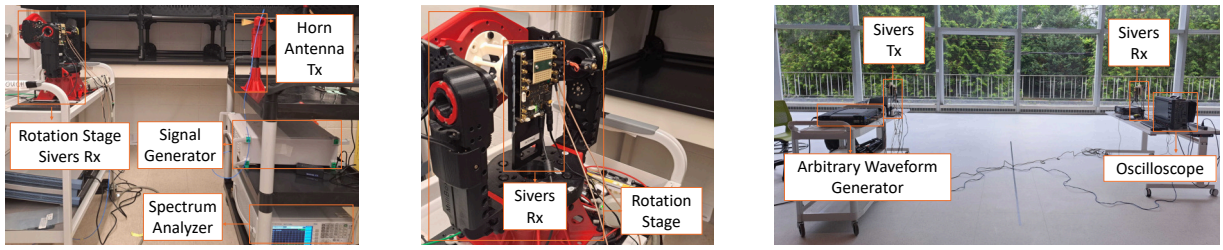

(a) (b) (c)

Figure 3: Experiment setup in EiCal: (a) radiation mapping (b) Rx details (c) Compressive sensing experiment.

where $m = min(N, K)$, $\sigma_i \geq 0$ are the singular values in decreasing order, $\mathbf{U}$ is an $N \times m$ orthonormal matrix containing the left singular vectors $\{\mathbf{u}_i, i = 1, ..., m\}$ as columns, $\mathbf{V}$ is an $K \times m$ orthonormal matrix containing the right singular vectors $\{\mathbf{v}_i, i = 1, ..., m\}$ as columns, with $\mathbf{x}^H$ denoting complex conjugate transposed of a vector or matrix $\mathbf{x}$. The best rank one approximation of $\mathbf{P}$ is known to be [5]

$$\widehat{\mathbf{P}} = \sigma_1 \mathbf{u}_1 \mathbf{v}_1^H \tag{9}$$

Comparing with (7) and ignoring the noise, we see that $\mathbf{u}_1$ should be proportional to $\mathbf{C}$ and $\mathbf{v}_1^H$ should be proportional to $(\alpha_1, ..., \alpha_K)$. Noting that proportionality constants do not matter for calibration and beamforming, we can therefore estimate the calibration vector as the first left singular vector:

$$\widehat{\mathbf{C}} = \mathbf{u}_1 \tag{10}$$

Once the calibration vector is estimated, any arbitrary desired beam pattern can be generated by simply first finding the corresponding nominal weight vector ($\mathbf{w}_{\text{des,nom}}$) using the theoretical array model, and then applying the calibration vector element-wise, as follows:

$$\mathbf{w}_{\text{des,cal}} = \hat{\mathbf{C}} \odot \mathbf{w}_{\text{des,nom}} \tag{11}$$

The weight vector thus obtained would be further quantized, depending on the hardware implementation of phased array control.

We will show in Sec. 5 that EiCal's calibration process is accurate even when only a small number of beams from the originally advertised codebook are employed. The quality of calibration improves with higher-resolution phase shifters yielding smaller quantization noise. Finally, we emphasize that in contrast to the conventional calibration methods that entail new measurements, EiCal does not require additional experiments to extract the calibration vector. Rather, it solely relies on the known codebook (even if it contains few beams) and the calculated weight vectors based on the theory of antenna and propagation. Therefore, EiCal offers a convenient way to generate accurate arbitrarily shaped beam patterns for various communication, sensing, and security scenarios.

4 IMPLEMENTATION AND BASELINES

We validate and evaluate the calibration accuracy of EiCal by employing commercial off-the-shelf mmWave arrays. Specifically, we use Sivers EVK06002 board [9], a 60GHz mmWave radio with 16×4 antennas. The manufacturer provides a codebook containing 63 weight vectors for each array, which can be used to create 63 different directional beams with the main lobe spanning -45 to 45 degrees in the azimuth direction with about 1.5 degrees step. The phase shifters have a 6-bit phase resolution and the distance between two array elements is slightly smaller than $\frac{\lambda}{2}$, which shows EiCal's ability to generalize to any phased array once its geometry is known.

Automated Radiation Mapping Setup. For evaluation purposes, we measure the radiation pattern of several custom beams and compared them against the calibrated simulation patterns. Our measurement setup is shown in Fig. 3a. On the right side, the transmitting horn antenna is shown which is directly facing the Sivers radio. The horn antenna is fed by a signal generator. On the RX side, we install the Sivers radio on the rotation stage with details in Fig. 3b. The stage is rotated from -90 degrees to 90 degrees with 2 degrees step. The Rx is directly connected to a spectrum analyzer. In all experiments, the center frequency is 60.48 GHz. We place signal absorbers (not shown) around the TX and RX to eliminate any potential multipath. In these experiments, we evaluate the calibration accuracy on the receiver phased array but the same methodology applies for transmitting arrays as well.

Calibration Baselines: We compare EiCal with the following baselines:

(a) No Calibration Vector. This baseline does not use any calibration vector to generate the beam pattern.

(b) Nulli-Fi [7]. This baseline finds the calibration vector by conducting multiple measurements such that all antennas are off except for two at each round. In each round, the relative phase between the two ON antennas is changed and the received signal amplitude is recorded. Clearly, the amplitude will be maximized when the two antennas become co-phase and the applied additional phase shift to make that happen infers the required phase calibration. By repeating the same procedure multiple rounds, one can obtain the relative phase shift for all antennas and form the calibration vector. Indeed, the main drawback of this scheme is that it requires exhaustive measurements in controlled settings.

Testing EiCal in Forming Desired Radiation Patterns: We evaluate the performance of EiCal in accurately generating custom desired beam patterns in practical settings:

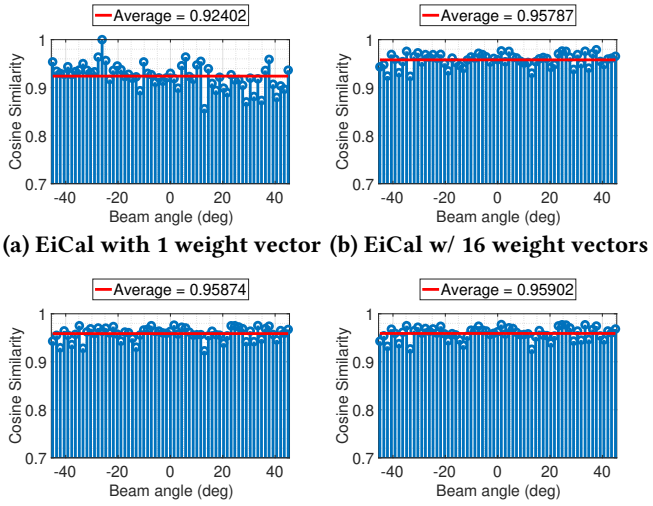

(a) EiCal with 1 weight vector (b) EiCal w/ 16 weight vectors

(c) EiCal w/ 32 weight vectors (d) EiCal w/ 63 weight vectors

Figure 4: Cosine similarities of estimated codebook after calibration with different methods.

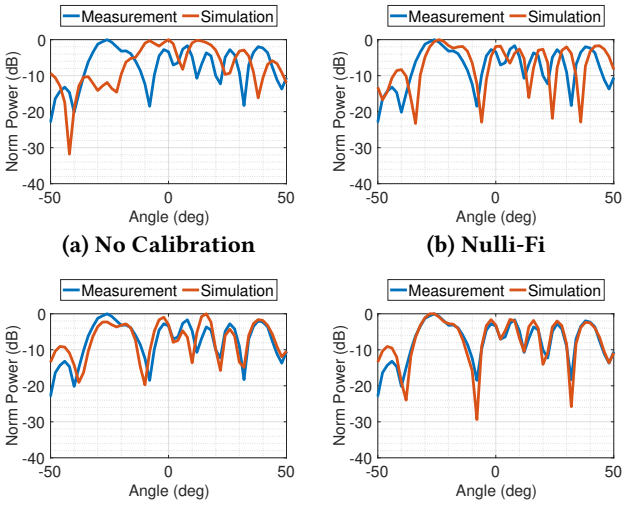

(a) No Calibration (b) Nulli-Fi

(c) EiCal with 1 weight vector (d) EiCal w/63 weight vectors

Figure 5: Compressive sensing beam patterns with different calibration methods.

(i) Compressive Beamforming. Compressive beamforming involves pseudo-random antenna weight vector selection (yielding a random-looking radiation pattern) and has shown to be an effective method for fast path discovery and angle of arrival estimation in mmWave networks [8]. However, the accuracy in angle estimation with compressive sensing depends on antenna calibration. Hence, we conduct experiments using the setup shown in Fig. 3c. The measurements are conducted in a large open space with a 3m Tx-Rx distance. Two Sivers radios act as Tx and Rx, which use omnidirectional beam and compressive sensing beam respectively. The Tx radio is connected to an arbitrary waveform generator(AWG), and the Rx radio is connected to an oscilloscope.

(ii) Null Steering. Null steering creates nulls in the direction of unintended users (or sources of interference) while steering the main lobe in the direction of target users. It has shown to be useful in minimizing interference and maximizing the Signal to Noise and Interference Ratio (SINR) in multi-user networks [2]. However, the null steering accuracy relies on antenna array calibration. Hence, we evaluate the performance of EiCal by investigating its role in nulling performance.

5 EVALUATION

5.1 Validity Assessment

As a first step, we evaluate how well we can reproduce the advertised codebook provided by the vendor with an estimated codebook produced using the extracted calibration vector. Specifically, we calculate cosine similarity, i.e.,

$$cos(\mathbf{a}_{\text{Adv}}(\Omega_k), \hat{\mathbf{a}}_{\text{Adv}}(\Omega_k)) = \frac{|\mathbf{a}_{\text{Adv}}(\Omega_k) \cdot \hat{\mathbf{a}}_{\text{Adv}}(\Omega_k)|}{\|\mathbf{a}_{\text{Adv}}(\Omega_k)\|_2 \|\hat{\mathbf{a}}_{\text{Adv}}(\Omega_k)\|_2}, \tag{12}$$

where $\hat{\mathbf{a}}_{\text{Adv}}(\Omega_k)$ is $\hat{\mathbf{a}}_{\text{Advertised}}(\Omega_k)$, the estimated steering vector obtained by substituting $\hat{\mathbf{C}}$ in Eq. (4). Fig. 4 depicts the cosine similarities between the advertised and estimated codebooks for our 60 GHz phased array when different numbers of beams are used for estimating the calibration vector. The x-axis shows the main lobe angle of the beams in the codebook (63 in total).

All cosine similarities are close to one, indicating that (1) array non-idealities are well modeled by a single calibration vector, and (2) the estimated calibration vector is closely aligned with the actual unknown calibration vector. Fig. 4 demonstrates that, while increasing the number of beams enhances the accuracy of the estimation, EiCal yields excellent results even when we use a small number of beams from the advertised codebook. This implies that the manufacturer can mitigate the tedious and costly process of antenna pattern measurement in an anechoic chamber as only a small number of beam measurements would suffice to find the calibration information. Furthermore, it suffices to report a single calibration vector to achieve performance comparable to that obtained by using a large codebook.

5.2 EiCal for Compressive Sensing

Compressive Sensing (CS) is a well-known technique that leverages the sparsity of the mmWave channels to reduce the number of required measurements for path discovery and fast beam establishment [8]. In traditional mmWave networks, the transmitter sweeps through a set of pre-defined directional beams and exploits feedback from the receivers to identify the best beam configuration and/or the dominant paths in the environment [4] [3]. CS-based beamforming, on the other hand, employs a fundamentally different approach. Instead of iterative feedback and adjustments, it uses a set of

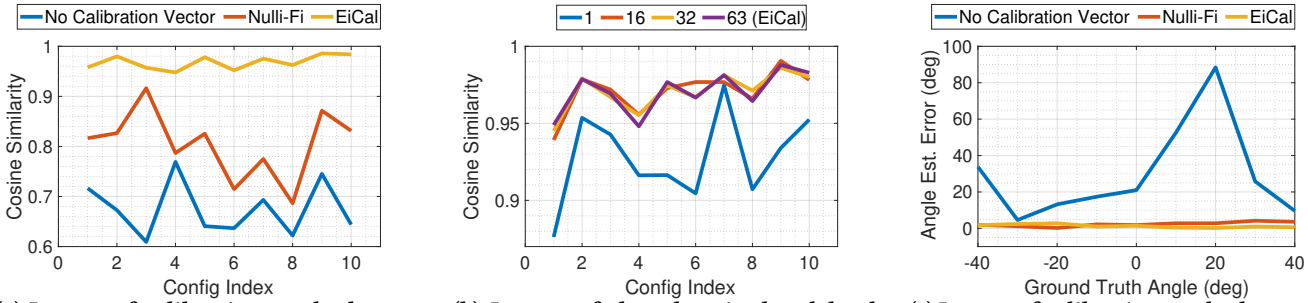

(a) Impact of calibration method on cosine similarity. **(b) Impact of the advertised codebook size on EiCal's performance.** **(c) Impact of calibration method on angle estimation error.**

Figure 6: Results of different calibration vectors on compressive sensing beam.

pseudorandom weight vectors to generate and transmit multiple beam patterns [8]. Then, the receiver extracts the sparse dominant channel components by assessing the correlation between the measured power and/or phase readings and the expected values of amplitude and phase over the suite of random yet known weight vectors. Obviously, any discrepancies between the actual transmitted radiation pattern and the theoretical pattern caused by calibration uncertainties would negatively impact the performance of compressive sensing.

5.2.1 Accurate Beam Generation. Fig. 5 depicts an example compressed beam (simulated vs measured beam pattern using a setup shown in Fig. 3) under four different calibration strategies. We observe that overall the simulated compressive sensing beam calibration vector from EiCal is the best match with the measurement patterns. We emphasize that the y-axis in Fig. 5 is in dB so even small visual discrepancies are significant.

To further evaluate the performance of our calibration method, we find the cosine similarity between simulated beam patterns and measured beam patterns for ten random compressive beam configurations. In order to compare beam patterns in this fashion, we represent each beam pattern by a vector corresponding to gains at angles spaced by 2 degrees, from -44 degrees to 44 degrees. We then compute the cosine similarity between these vectorized beam patterns. Fig. 6a illustrates the result in which the x-axis represents different configuration indices, while the y-axis shows the cosine similarity. Higher cosine similarity values indicate better performance, as they signify that the generated beam pattern is more similar to the ideal pattern. The EiCal consistently achieves higher cosine similarity values compared to other baseline methods, demonstrating its effectiveness in producing accurate beam patterns. We repeat the cosine similarity analysis for EiCal but this time the calibration vector is extracted using fewer beams in the advertised codebook. Fig. 6b reveals a consistently high cosine similarity can be achieved even with 16 beams. This implies that the manufacturer can indeed reduce the cost of codebook generation by only measuring a few beams in an anechoic chamber.

5.2.2 Angle Estimation Performance. We now evaluate the performance of our calibration scheme in CS-based angle estimation, using the noncoherent compressive sensing method in [8]. We place the TX in different angular locations relative to the RX which employs various randomly generated CS beams and records the measured amplitude or power. CS-based angle estimation algorithm finds the angle of arrival for which the pattern of measured power fluctuations across different CS beams has the highest correlation with the corresponding nominal power fluctuations. Hence, it is evident that under a perfectly calibrated array, the error of such angle estimation is minimal.

Fig. 6c shows the estimated angle error with different calibration methods across radio field of view. The x-axis represents different ground truth angles for TX, while the y-axis shows the estimated angle error in degrees. Without calibration, the angle estimation error is very high, as expected. The average angle error for Null-Fi and EiCal is 2.31 and 1.29 degrees, respectively. Thus, EiCal provides better angle estimation performance while eliminating the need for exhaustive measurements.

These results highlight the effectiveness of EiCal in creating accurately predictable arbitrary pseudorandom beams leading to improved localization performance.

5.3 EiCal for Null Steering

Null forming and steering are known beam manipulation techniques that help with interference management in wireless networks. For instance, by creating nulls in the direction of unintended users, one can mitigate the interference of multi-user communication. Null steering is also used in the context of wireless security by minimizing the radiated energy in space toward the direction of a potential eavesdropper. Any null steering algorithm requires a well-calibrated array to function effectively, i.e., to ensure that the signals emitted from different antennas add up destructively in the desired null direction.

5.3.1 Setup. To assess the performance of EiCal in creating null patterns, we implemented an algorithm from the literature known as Mambas [2] in our mmWave setup. This

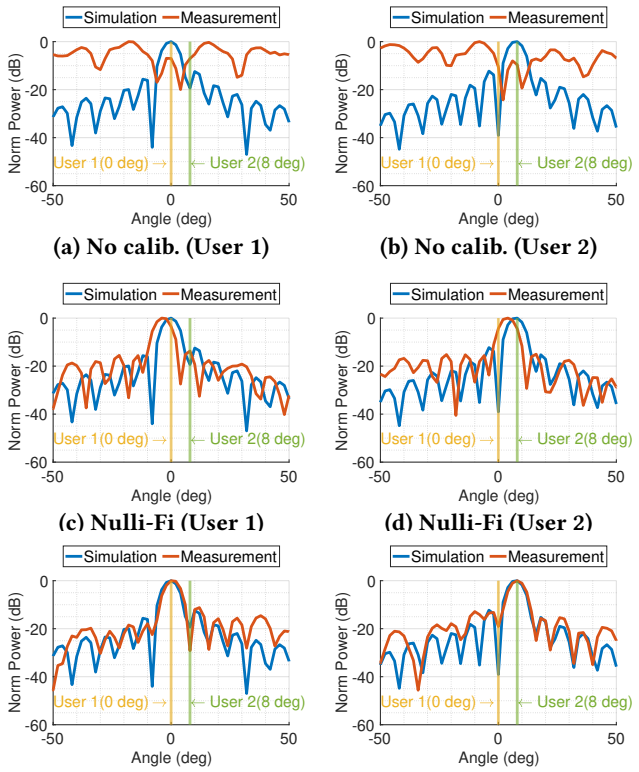

(a) No calib. (User 1) (b) No calib. (User 2)

(c) Nulli-Fi (User 1) (d) Nulli-Fi (User 2)

(e) EiCal (User 1) (f) EiCal (User 2)

Figure 7: Null steering performance with different calibration vectors and users.

algorithm steers the beam toward the desired user while creating nulls toward other users, thereby maximizing the SINR. Mambas serves a set of users in each time slot, optimizing the beamforming coefficients to enhance user-specific signal quality and interference suppression. We conduct measurements using a similar setup explained in Sec. 4. Two users transmit their signal toward the RX equipped with mmWave phased array. The RX performs null forming to maximize the received SINR of user 1 (user 2 is the source of interference) and vice versa.

Fig. 7 compares the null steering performance of different calibration schemes. In this configuration, we consider an uplink scenario with two closely spaced users, separated by 8°. As expected, the results show that null steering is not feasible without calibration. The results in Fig. 7e and 7f demonstrate that with EiCal, the antenna array is well-calibrated, enabling effective beamforming and null steering. Conversely, Fig. 7c and 7d show that the Nulli-Fi calibration yields misaligned main lobe and null directions.

5.3.2 Analysis. To further evaluate the performance of EiCal scheme, we use two key metrics: *(i)* cosine similarity between measured and simulation patterns and *(ii)* peak to null power ratio. Fig. 8 demonstrates these metrics for EiCal compared to baseline methods across the ground truth (GT) nulling angles. First, from Fig. 8a, it is evident that successful null steering does indeed require calibration. In this figure, the x-axis represents different configurations, i.e., different users' locations. Without any calibration, the cosine similarity is pretty low. The average cosine similarity for Null-Fi and EiCal is 0.9363 and 0.9536, respectively. The EiCal scheme achieves the highest cosine similarity without additional experiments, unlike the measurement-heavy Null-Fi approach.

Fig. 8b and 8c illustrate the peak-to-null power ratio in dB. The x-axis represents the GT nulling angles in degrees. Larger values indicate better performance, as they signify that interference at the nulling angle is better mitigated. We show both the median and worst null performance. Worst nulling performance captures the minimum peak-to-null power ratio within 4 degrees of the target GT null angle. Median nulling performance captures the median of the peak-to-null power ratio within 4 degrees of the GT null angle. The average median nulling performance for Nulli-Fi, and EiCal is 15.4605 dB, 19.9891 dB, respectively. The average worst nulling performance for Nulli-Fi, and EiCal is 12.7851 dB and 16.7440 dB, respectively. It is evident that EiCal outperforms Null-Fi in null steering performance. EiCal does so while being a zero-shot and measurement-free scheme.

6 RELATED WORK

Analog beam manipulation has been well explored in the past literature in several domains including wireless communication, sensing, and security. Existing works either rely on the provided codebook by the manufacturer to create pre-defined beam patterns [11], manipulate the codebook to create a limited number of new beam patterns (e.g., two-lobe beams) [12], or perform exhaustive calibration to generate on-demand arbitrary patterns [6].

Existing efforts for array calibration include brute force measurements such as changing the phase of two antennas [7], setting the array in beam steering mode [10], or measuring the impact on amplitude and phase upon reversing the phase for each element [13]. Unfortunately, such schemes are time-consuming and do not scale well. More importantly, they do not apply for calibrating arrays that are already deployed in the wild, since doing controlled measurements (e.g., without multipath and with accurate alignment) is not straightforward. We have implemented one such recent approach [7] as a baseline, and shown that it is outperformed by EiCal.

Compared to this prior work, EiCal is accurate, zero-shot, and experiment-free. EiCal only takes the geometry of the array and the directional codebook provided by the manufacturer as the input. Our extensive simulation and experimental demonstrations in various tasks, including compressive sensing and null steering, show that EiCal achieves accurate performance while being lightweight and scalable.

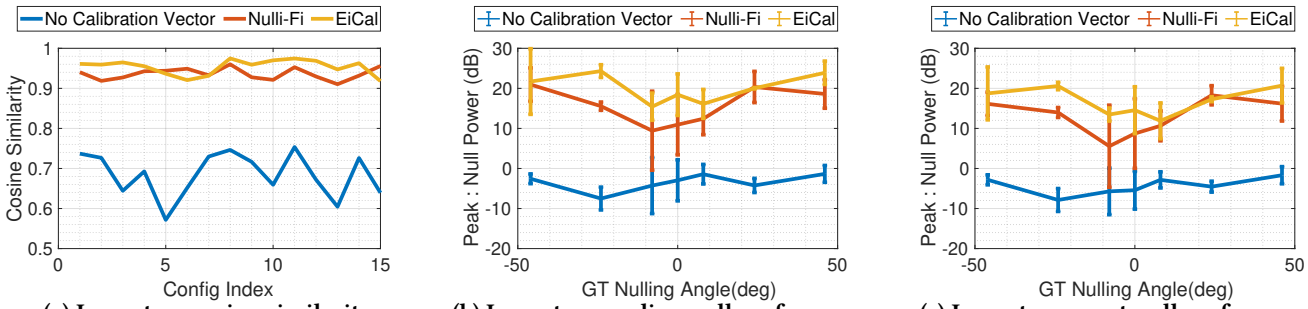

(a) Impact on cosine similarity. **(b) Impact on median null performance.** **(c) Impact on worst null performance.**

Figure 8: Results of different calibration methods on null beam.

7 CONCLUSION AND FUTURE WORK

This paper presents EiCal, an accurate, zero-shot calibration scheme that solely exploits knowledge of array geometry and the directional codebook advertised by the manufacturer, using eigen-analysis to obtain an accurate calibration vector *without the need for additional measurements*. We experimentally evaluate EiCal on off-the-shelf 60 GHz arrays showing that our calibration vector enables the accurate generation of diverse beam patterns beyond basic beamforming in a specified direction, including pseudorandom compressive beams with applications in localization, and null steering for interference management. Our findings also indicate that we can substantially decrease the number of entries in the codebook without compromising the quality of the extracted calibration vector, potentially reducing the burden of calibration in the manufacturing process. Future work may explore the extension of this method to other phased array geometries and hardware configurations. Additionally, integrating this calibration approach with adaptive beamforming techniques could provide even greater flexibility and performance in dynamic communication environments.

ACKNOWLEDGMENTS

This work was supported in part by the National Science Foundation (grants 2148271, 2148303 and 2215646) and by the Center for Ubiquitous Connectivity (CUbiC), sponsored by Semiconductor Research Corporation (SRC) and Defense Advanced Research Projects Agency (DARPA) under the JUMP 2.0 program.

REFERENCES

[1] Benjamin Friedlander. 2018. Antenna Array Manifolds for High-Resolution Direction Finding. *IEEE Transactions on Signal Processing* 66, 4 (2018), 923–932. https://doi.org/10.1109/TSP.2017.2778683

[2] Zhihui Gao, Zhenzhou Qi, and Tingjun Chen. 2024. Mambas: Maneuvering Analog Multi-User Beamforming using an Array of Subarrays in mmWave Networks. In *Proceedings of the 30th Annual International Conference on Mobile Computing and Networking*. 694–708.

[3] Yasaman Ghasempour, Claudio R. C. M. da Silva, Carlos Cordeiro, and Edward W. Knightly. 2017. IEEE 802.11ay: Next-Generation 60 GHz Communication for 100 Gb/s Wi-Fi. *IEEE Communications Magazine* 55, 12 (2017), 186–192.

[4] Yasaman Ghasempour, Muhammad K. Haider, Carlos Cordeiro, Dimitrios Koutsonikolas, and Edward Knightly. 2018. Multi-Stream Beam-Training for mmWave MIMO Networks. In *Proceedings of the 24th Annual International Conference on Mobile Computing and Networking (MobiCom '18)*. Association for Computing Machinery, 225–239.

[5] R. A. Horn and C. R. Johnson. 2012. *Matrix Analysis*. Cambridge University Press.

[6] Jesus Omar Lacruz, Dolores Garcia, Pablo Jiménez Mateo, Joan Palacios, and Joerg Widmer. 2020. mm-FLEX: an open platform for millimeter-wave mobile full-bandwidth experimentation. In *Proceedings of the 18th International Conference on Mobile Systems, Applications, and Services*. 1–13.

[7] Sohrab Madani, Suraj Jog, Jesus O Lacruz, Joerg Widmer, and Haitham Hassanieh. 2021. Practical null steering in millimeter wave networks. In *18th USENIX Symposium on Networked Systems Design and Implementation (NSDI 21)*. 903–921.

[8] Maryam Eslami Rasekh, Zhinus Marzi, Yanzi Zhu, Upamanyu Madhow, and Haitao Zheng. 2017. Noncoherent mmWave path tracking. In *Proceedings of the 18th International Workshop on Mobile Computing Systems and Applications*. 13–18.

[9] Sivers Semiconductors. 2024. *Evaluation Kit EVK06002*. Retrieved July 26, 2024 from https://www.sivers-semiconductors.com/5g-millimeter-wave-mmwave-and-satcom/wireless-products/evaluation-kits/evaluation-kit-evk06002/

[10] Zhengpeng Wang, Fengchun Zhang, Huaqiang Gao, Ondrej Franek, Gert Frølund Pedersen, and Wei Fan. 2021. Over-the-air array calibration of mmWave phased array in beam-steering mode based on measured complex signals. *IEEE Transactions on Antennas and Propagation* 69, 11 (2021), 7876–7888.

[11] Qian Yang, Hengxin Wu, Qianyi Huang, Jin Zhang, Hao Chen, Weichao Li, Xiaofeng Tao, and Qian Zhang. 2023. Side-lobe can know more: Towards simultaneous communication and sensing for mmWave. *Proceedings of the ACM on Interactive, Mobile, Wearable and Ubiquitous Technologies* 6, 4 (2023), 1–34.

[12] Chao Yu, Yifei Sun, Yan Luo, and Rui Wang. 2023. mmAlert: mmWave Link Blockage Prediction via Passive Sensing. *IEEE Wireless Communications Letters* (2023).

[13] Fengchun Zhang, Wei Fan, Zhengpeng Wang, Yusheng Zhang, and Gert F Pedersen. 2019. Improved over-the-air phased array calibration based on measured complex array signals. *IEEE Antennas and Wireless Propagation Letters* 18, 6 (2019), 1174–1178.

[14] Jing Zhang, Xiaohu Ge, Qiang Li, Mohsen Guizani, and Yanxia Zhang. 2016. 5G millimeter-wave antenna array: Design and challenges. *IEEE Wireless communications* 24, 2 (2016), 106–112.

[15] Dixian Zhao, Peng Gu, Jiecheng Zhong, Na Peng, Mengru Yang, Yongran Yi, Jiajun Zhang, Pingyang He, Yuan Chai, Zhihui Chen, et al. 2021. Millimeter-wave integrated phased arrays. *IEEE Transactions on Circuits and Systems I: Regular Papers* 68, 10 (2021), 3977–3990.